Water Research 188 (2021) 116508

Contents lists available at ScienceDirect

Water Research

journal homepage: www.elsevier.com/locate/watres

Redox condition of saline groundwater from coastal aquifers influences reverse osmosis desalination process

Shaked Stein[a,b,c], Orit Sivan[a,*], Yoseph Yechieli[c,d], Roni Kasher[b,*]

[a] The Department of Earth and Environmental Sciences, Ben-Gurion University of the Negev, Beer Sheva 84105, Israel
[b] Department of Desalination and Water Treatment, Zuckerberg Institute for Water Research, Jacob Blaustein Institutes for Desert Research, Ben-Gurion University of the Negev, Sede Boqer Campus, Midreshet Ben-Gurion, 8499000, Israel
[c] Geological Survey of Israel, 32 Yesha'ayahu Leibowitz, Jerusalem 9692100, Israel
[d] Department of Environmental Hydrology and Microbiology, Zuckerberg Institute for Water Research, The Blaustein Institutes for Desert Research, Ben-Gurion University of the Negev, Sde Boqer Campus, Midreshet Ben-Gurion, 8499000, Israel

ARTICLE INFO

Article history:
Received 2 July 2020
Revised 29 September 2020
Accepted 8 October 2020
Available online 9 October 2020

Keywords:
Saline groundwater
Reverse osmosis
Redox
Seawater desalination
Coastal aquifers

ABSTRACT

Reverse osmosis (RO) seawater desalination is a widely applied technological process to supply potable water worldwide. Recently, saline groundwater (SGW) pumped from beach wells in coastal aquifers that penetrate beneath the freshwater-seawater interface is considered as a better alternative water source to RO seawater desalination as it is naturally filtered within the sediments which reduces membrane fouling and pre-treatment costs. The SGW of many coastal aquifers is anoxic – and thus, in a low redox stage – has elevated concentrations of dissolved manganese, iron and sulfides. We studied the influence of the SGW redox stage and chemistry on the performance - permeate flux and fouling properties - of RO desalination process. SGWs from three different coastal aquifers were sampled and characterized chemically, and RO desalination experiments were performed under inert and oxidized conditions. Our results show that all three aquifers have anoxic saline groundwater and two of them have intensive anaerobic oxidation of organic matter. Two aquifers were found to be in the denitrification stage or slightly lower and the third one in the sulfate reduction stage. Our results indicate that the natural redox stage of SGWs from coastal aquifers affects the performance of RO desalination. All SGW types showed better RO performance over seawater desalination. Furthermore, air oxidation of the SGW was accompanied with pH elevation, which increased the membrane fouling. Hence, keeping the feed water unexposed to atmospheric conditions for maintaining the natural reducing stage of the SGW is crucial for low fouling potential. The observed benefits of using naturally reduced SGW in RO desalination have significant implications for reduction in overall process costs.

1. Introduction

Current global water scarcities are forecasted to worsen in the near future (Greve et al., 2018) as freshwater resources become depleted due to ongoing overexploitation and contamination, especially in arid and semi-arid regions (Hoekstra and Mekonnen, 2012). A key technology for coping with the freshwater shortage is reverse osmosis (RO) desalination, which accounts for almost 70% of the global desalination capacity (Amy et al., 2017). On a global scale, about 60% of the feed water for desalination is seawater, 23% is brackish water, and the remainder comprises wastewater and other sources (Shahzad et al., 2017).

Saline groundwater (SGW) from coastal aquifers is an alternative source for seawater desalination (Dehwah and Missimer, 2016; Sola et al., 2013; Stein et al., 2016), as it possesses a reduced fouling propensity due to the natural filtration it undergoes through the porous media (Stein et al., 2016). Moreover, its use leads to decreased greenhouse gas emissions due to lower energy consumption (Dehwah and Missimer, 2016) and reduced process costs than are required in conventional seawater desalination. SGW is the saline water body in a coastal aquifer that is naturally created by seawater intrusion, which is in hydrodynamic equilibrium with the freshwater body above it. The natural dynamic of the fresh-saline water interface (FSI) (Andersen et al., 2005; Michael et al., 2005; Yechieli et al., 2010) in many coastal aquifers is altered by the overexploitation of the fresh groundwater, and this pushes the FSI further inland (Houben and Post, 2017; Zhou et al., 2005), thereby salinizing the groundwater and degrading its quality. Pumping

* Corresponding authors.
E-mail addresses: shakedstein@gmail.com (S. Stein), oritsi@bgu.ac.il (O. Sivan), kasher@bgu.ac.il (R. Kasher).

https://doi.org/10.1016/j.watres.2020.116508
0043-1354/

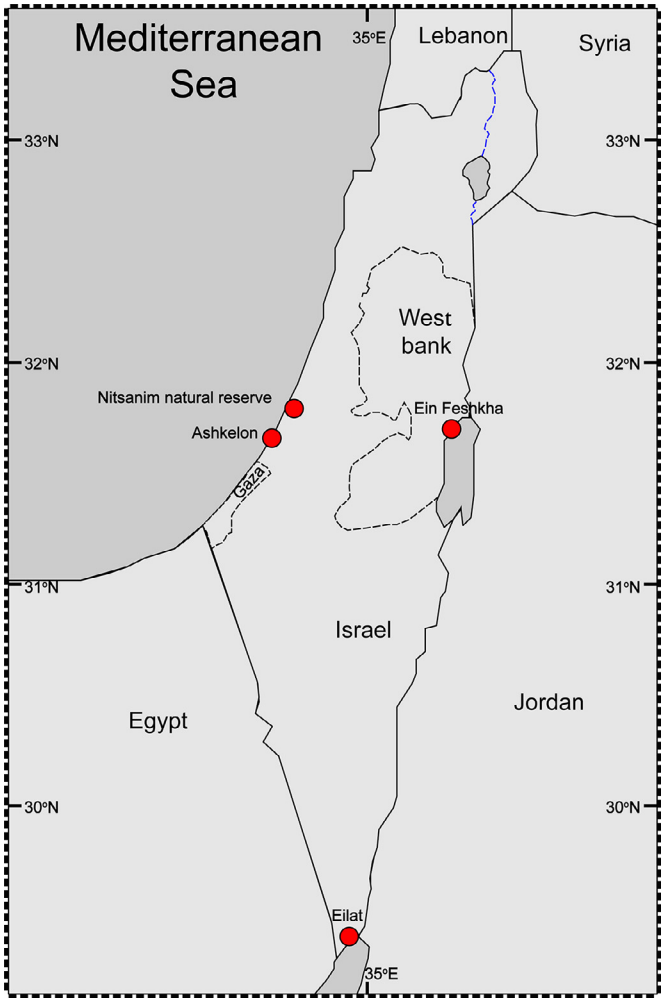

Fig. 1. Locations of the study sites. Red circles represent sampling locations for the desalination experiments.

SGW from a coastal aquifer as feed for desalination plant was shown to shift the FSI toward the well, thus freshening and rehabilitating the aquifer in its vicinity (Stein et al., 2019,2020).

The membranes used in RO desalination suffer from fouling, the deposition and accumulation of substances on the membrane surface. Membrane fouling is especially problematic for RO and nanofiltration technologies, in which backwashing is not applicable. Fouling, which increases the membrane's hydraulic resistance and reduces its overall performance, may comprise colloidal or mineral deposition (scaling), adherence of organics, or biofilm growth (biofouling) (Sim et al., 2018). To improve the RO process and reduce its operational costs, it is critical to find an efficient solution to membrane fouling.

Understanding the influence of SGW chemistry on the desalination performance is crucial for reducing membrane fouling in SGW desalination. Specifically, the reduction-oxidation (redox) stage of SGW differs from that of seawater, and its effect on the desalination process is not fully understood. The FSI often manifests as an oxycline, wherein the upper freshwater part is oxidized while the SGW is oxygen depleted (Russak et al., 2015; Sivan et al., 2005). The exhaustion of the oxygen in the saline zone causes anaerobic metabolism to dominate, using other electron acceptors according to their energy yields (Stumm and Morgan, 2012). A variety of redox stages of the SGW that are driven by denitrification, the reductive dissolution of manganese and iron oxide minerals, sulfate reduction and finally methanogenesis (with the lowest redox stage), are found around the world (Charette et al., 2005; Connor et al., 2015; Kim et al., 2014; Porubsky et al., 2014; Roy et al., 2010; Santos et al., 2011; Snyder et al., 2004). A previous study showed reductive dissolution of iron and manganese in saline groundwater of coastal environments (Duncan and Shaw, 2003). Furthermore, near the FSI, the redox stage is altered due to oscillations in the interface level at which dissolved iron is precipitated when the environment becomes oxic (Sirois et al., 2018). Moreover, another study found that the presence of natural organic matter in the groundwater enhances the rate of iron reduction (Chen et al., 2003).

The use of anaerobic groundwater as feed water for desalination may enhance fouling because upon exposure of the effluents to atmospheric oxygen, dissolved iron and sulfur may precipitate as sulfur and iron oxides. At a desalination plant in Bahrein, colloidal sulfur concentrations of 5 ppm in anoxic raw water caused severe fouling in the pretreatment cartridge filters and in the RO membranes by sulfur deposits within two days of operation (Ning et al., 2005). At a desalination plant in Fort Myers, nanofiltration treatment of anoxic groundwater was affected by particle fouling due to the precipitation of iron hydroxide and elemental sulfur (Nederlof et al., 2000). In laboratory experiments, researchers found that the addition of reduced iron to oxic feed water resulted in the rapid precipitation of iron oxides and extensive membrane fouling (Yiantsios and Karabelas, 2003). Hence, the unique redox conditions of saline groundwater may affect the RO process and membrane fouling behavior.

The aim of the present study was to investigate how the natural redox stage of the SGW from coastal aquifers affects the performance of the RO desalination process. We sampled and characterized the SGW of three different coastal zones – the Eastern Mediterranean, the Red Sea and the Dead Sea coastal aquifers – with potentially different compositions and redox stages. RO desalination experiments of the different SGW types were then carried out to test the performance and fouling characteristics of the process. Additionally, different exposures of the feed water to atmospheric oxygen were tested, and the effects on the water chemistry and fouling behavior were examined. To the best of our knowledge, this study provides the first insight on desalination of naturally reduced saline groundwater in coastal regions and its implications for control of membrane fouling.

2. Methods

2.1. Sampling Sites

2.1.1. The Eastern Mediterranean coastal aquifer (Nitsanim nature reserve)

The Nitsanim Nature Reserve is located on the southern part of the coastal plain of Israel (Fig. 1). The well that was used for this study (112-W) is located 230 m from shore and is 55 m deep. It cuts through the sandy cross section, while the well screen is located at depths of 18 to 55 m.

2.1.2. The Red Sea coastal aquifer (Eilat area)

The water for this research was sampled from an observation well (Meridian T-1) that is located ~20 m from the shore (Fig. 1) and that is 117 m deep. The well is screened 30 m from a depth of 84 m to 114 m, representing the lower confined aquifer.

2.1.3. The Dead Sea coastal aquifer (Ein Feshkha nature reserve)

The groundwater for this study was sampled from an observation well (EZ-112) that is an artesian well. The well is cut through the alluvial aquifer of the Dead Sea (Fig. 1) to a depth of 40 m and is screened at depths of 31 to 36 m in a gravel layer. That layer is confined by upper and lower impermeable clay layers with thicknesses of 3 and 1 m, respectively.

Seawater from the desalination plant in Ashkelon (Fig. 1) was also sampled and examined. The desalination plant started operating in 2006 and produces 100 million $m^3\ y^{-1}$ of potable water. The supplementary materials include detailed descriptions of the different sampling sites and aquifers.

2.2. Water sampling and field procedures

SGW in the Nitsanim and Eilat sampling campaigns was collected with a submersible pump (Grundfos, Bjerringbro, Denmark). In the Ein Feshkha (Dead Sea) sampling campaign, a pump was not needed due to the artesian nature of the well. Seawater was collected from the inlet of the Ashkelon desalination plant to sample the feed water source of an industrial seawater desalination plant. SGW was sampled in an inert environment by collecting the water in a 200-L tank filled with nitrogen gas; during water sampling the gas was released from the tank through an outlet pipe and a gas trap. For Eilat and Ein Feshkha waters, half of the sampled volume (100 L) was kept inert as described, and the other half was oxidized by opening the tank and stirring for 24 h to evaluate the effects of exposure of the water to atmospheric conditions.

Parameters that were measured on site in each sampling campaign included electrical conductivity (EC), pH, dissolved oxygen (DO), and temperature, which were measured using the Multi 3620 IDS (WTW, Germany), and oxidation–reduction potential (ORP), which was measured using a Quatro Professional Plus instrument (YSI, USA). The silt density index (SDI) was also measured on site by filtering the water through a 0.45-μm filter at 30 psi for 15 min using the SDI-2000 portable test kit (Applied membranes, Inc. USA). Subsamples were prepared using different protocols after filtering the water through a 0.22-μm filter (Millex): Subsamples for trace metals were acidified to pH 2 with 70% nitric acid purified by redistillation (Aldrich). Subsamples for alkalinity, dissolved inorganic carbon (DIC) and nutrients analyses were preserved unacidified, and the samples for NH_4^+, NO_2^- and NO_3^- were kept at −20 °C until analysis. Subsamples for ferrous iron and sulfide analyses were treated immediately using a ferrozine solution and zinc acetate, respectively, in separate vials. Subsamples for total organic carbon (TOC) were not pre-filtered.

2.3. Water chemical analyses

Na^+, Ca^{2+}, Mg^{2+}, K^+, Sr^{2+}, Mn and boron were analyzed by inductively coupled plasma-optical emission spectroscopy (ICP-OES) using the Spectro Arcos instrument (Kleve, Germany). Cl^-, Br^- and SO_4^{2-} were analyzed by ICS-5000 ion chromatograph (Dionex, Thermo Fisher Scientific). Alkalinity was analyzed by titration by Titrino 785 (Metrohm, Herisau, Switzerland) using 0.01 N HCl solution with a precision of 1%. DIC and its isotopic composition ($\delta^{13}C_{DIC}$) were analyzed on a DeltaV Advantage isotop-ratio mass-spectrometer (Thermo Fisher Scientific) at a precision of ±0.1‰. TOC was measured with Sievers InnovOx ES Laboratory TOC Analyzer (Trevose, PA, USA) with 3% precision and a detection limit of 0.5 ppm using a persulfate with non-dispersive infrared (NDIR) detector. Ferrous iron fixed with ferrozine (Stookey, 1970) was measured at 562 nm on a spectrophotometer with a detection limit of 1 µmol L^{-1}. Sulfide was measured using the Cline method (Cline, 1969) by reading the absorbance at 665 nm with a detection limit of 1 µmol L^{-1}.

2.4. Reverse osmosis filtration experiments

RO filtration experiments were conducted to evaluate the extent of fouling in the different water types (see Table 1) using a flat-sheet RO membrane (SW30HR, Dow-FILMTEC) at a constant pressure while monitoring the permeate flux decline. The RO filtration system is shown schematically in Fig. 2. The large water tank (200 L) of SGW or seawater sampled in the field was kept in an inert atmosphere (N_2) during the sampling and during the filtration experiment, and was mixed by a small circulation pump immersed in the tank. For the oxidized waters, no nitrogen atmosphere was applied. The filtration system was operated in a 'feed and bleed' mode: Feed water was pumped from the 200-L tank at 100 mL min^{-1} into the RO system by a peristaltic pump (MRC), while the permeate and concentrate were recycled back into a small water tank (10 L; Fig. 2). Water was drained from the small tank at a rate (flux equal to the inlet flux, 100 ml min^{-1}) that maintained a constant volume of the feed solution (4 L) in the tank. The temperature was controlled using a heat exchange unit and was set to 25 ºC. The RO system comprised a rectangular flat-sheet pressure cell (Sterlitech, 12.7 × 10 cm^2; membrane dimensions 8.5 × 3.8 cm^2), a Flomega flow meter (Brooks instruments, Hatfield, PA USA) for the permeate, a high-pressure pump, a secondary pump, and a cartridge filter (10 µm). In all filtration experiments, the initial permeate flow was set to ~100 g h^{-1} (flux of 30.5 L $m^{-2}\ h^{-1}$) by adjusting the applied pressure (in a range of 40 to 50 bars), and the duration of the experiments was ~8 h. Additionally, the feed–brine circulation flow was set to 1.3 L min^{-1} (cross flow velocity of 0.24 m sec^{-1}) to obtain an overall similar ratio between the shear and the drag forces on the membrane.

2.5. Membrane autopsy

On the completion of each experiment the fouled membranes were cut into pieces of 2 × 2 cm and dried under vacuum at room temperature for surface analyses. For chemical analyses of the deposits, membrane pieces from each experiment were immersed in 3 mL of 1 M HNO_3 solution and shaken overnight on an orbital shaker. Chemical analyses were performed by ICP-OES. Surface elemental compositions were detected by X-ray photoelectron spectroscopy (XPS) ESCALAB 250 (Thermo Fisher™ Scientific Inc., Waltham, UK) using an Al X-ray source and a monochromator. The morphologic features of the fouled membrane surfaces were studied using the QUANTA 200 scanning electron microscope (SEM; Thermo Fisher™ Scientific Inc., Waltham, UK) along with energy dispersive X-ray spectroscopy (EDS) analysis to detect the chemical compositions of specific particles.

3. Results and discussion

3.1. Water chemistry and redox conditions

SGW from three different coastal aquifers and seawater from the intake pipe of the Ashkelon desalination plant (prior to treatment) were sampled (Fig. 1). All SGWs were sampled several meters below the FSI, and their water chemistries were analyzed (Table 1). The average salinity measurement (total dissolved solids, TDS) for all the SGW samples was around 30 ppt, compared with the 42 ppt of the Eastern Mediterranean seawater, indicating some mixing with the fresh groundwater body. The slightly lower average salinity observed in the SGW samples, which was close to that of the nearby seawater, is typical to the levels of salinity in many other SGWs from coastal aquifers around the world (Russak and Sivan, 2010; Sivan et al., 2005; Yechieli et al., 2009).

The ion concentrations of the SGW from all three aquifers were, however, deviated from simple mixing with fresh groundwater. The simple mixing was calculated using the concentration of the Cl^- ion (see SI, equation S5), which was shown to be a conservative chemical specie in those coastal aquifers and mimics the TDS of the water (Avrahamov et al., 2010; Russak and Sivan, 2010). Among the non-conservative ions in the SGW are Ca^{2+}, Na^+, K^+ and Sr^{2+}.

Table 1
Physicochemical properties of the different water types that were used in the desalination experiments. All values are in millimolar [mM] units unless stated differently.

	SW	Nitsanim	Eilat	Eilat oxidized	Ein Feshkha	Ein Feshkha oxidized
EC [mS cm^{-1}]	56.1[b]	47[b]	33[b]	34	39.9[b]	41
pH	8.27[b]	7.3[b]	7.06[b]	7.5	6.75[b]	7.7
Temp[b] [°C]	21.7	23.2	31	ND[a]	31	ND
SDI[b] [% min^{-1}]	6.35	4.6	5.44	ND	0.91	ND
TDS [ppt]	41.8	33.9	22.5	23.6	24.7	25.3
B	0.5	0.26	0.25	0.27	0.68	0.67
Ca^{2+}	11.45	15.2	15.1	15.3	34.65	31.8
Ba^{2+} [μM]	BDL[a]	0.4	BDL	BDL	2	2
K^{+}	13.3	7.5	4.5	4.6	17.5	17.4
Mg^{2+}	64.7	43.6	29.9	30.4	121.8	114
Na^{+}	592	460	294	307	217.6	204
Sr^{2+}	0.09	0.11	0.32	0.33	0.22	0.2
Si	BDL	0.15	0.51	0.53	0.29	0.29
Alkalinity	2.6	3.4	2.4	2.7	4.2	1.5
Cl^{-}	638	526	327	349	493	477
Br^{-}	1.3	1.3	0.23	0.28	4.5	4.4
SO_4^{2-}	30	25	25.1	25.4	1.8	1.8
ORP[b] [mV]	−5	−60	−103	ND	−230	ND
DO [mg L^{-1}]	9.01[b]	0.13[b]	0.06[b]	8.6	0.07[b]	8.6
NO_2^{-} [μM]	0.1[c]	0.9	0.47	ND	0.6	ND
NO_3^{-} [μM]	0.3[d]	80	50	ND	0.1	ND
NH_4^{+} [μM]	1[d]	2.4	0.58	ND	4.5	ND
Total Mn [μM]	BDL	BDL	BDL	BDL	1.4	1.5
Fe^{2+}[μM]	BDL	BDL	BDL	BDL	4.3	BDL
HS^{-} [μM]	BDL	BDL	BDL	BDL	32.2	1.53
DIC	2.6	3.6	2.4	2.8	4.7	1.7
$\delta^{13}C_{DIC}$ [‰]	−0.7	−5.7	−1.4	−0.4	−7.9	−2.55
TOC [ppm]	1.12	0.6	BDL	ND	2	ND

[a] ND, not determined; BDL, Below detection limit.
[b] Parameter measured on site.
[c] Taken from (Krom et al., 2005).
[d] Taken from (Sivan et al., 2005).

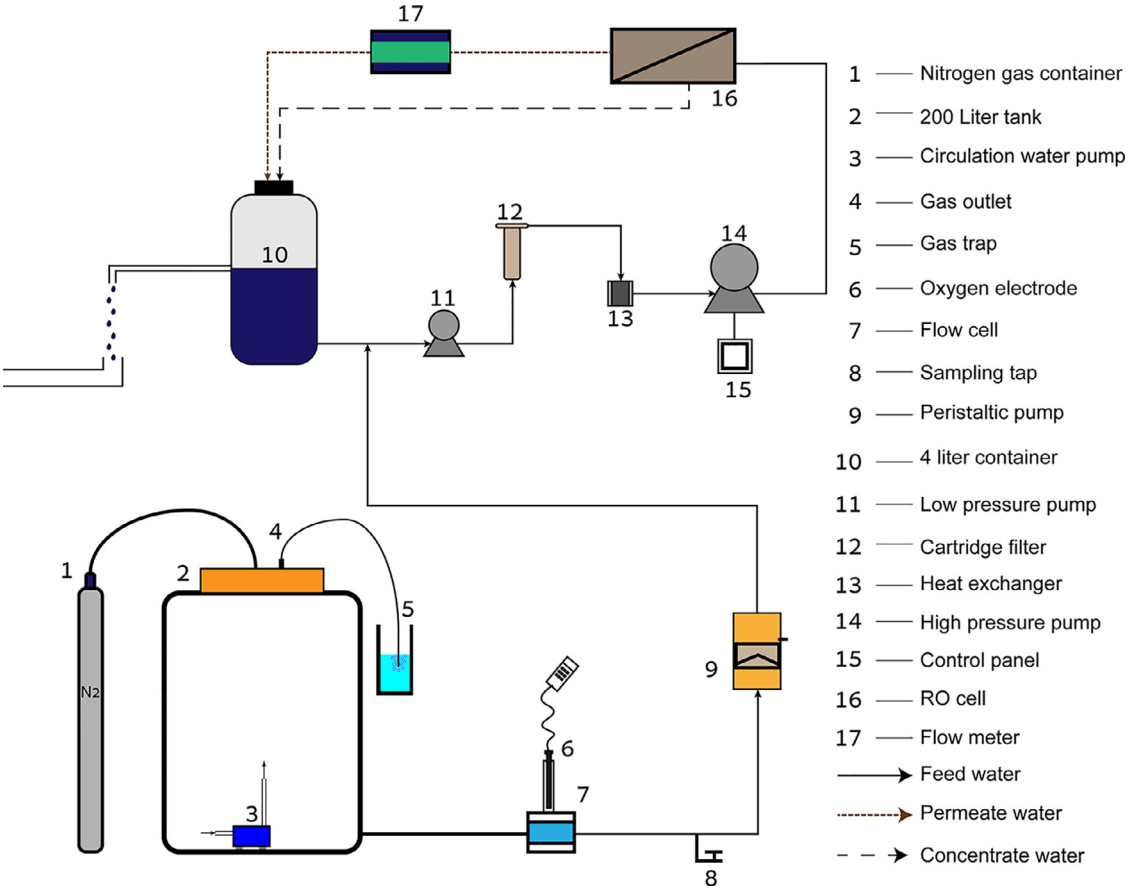

Fig. 2. Schematic of the reverse osmosis cross flow filtration system for evaluating the fouling and system performance with the difference water types.

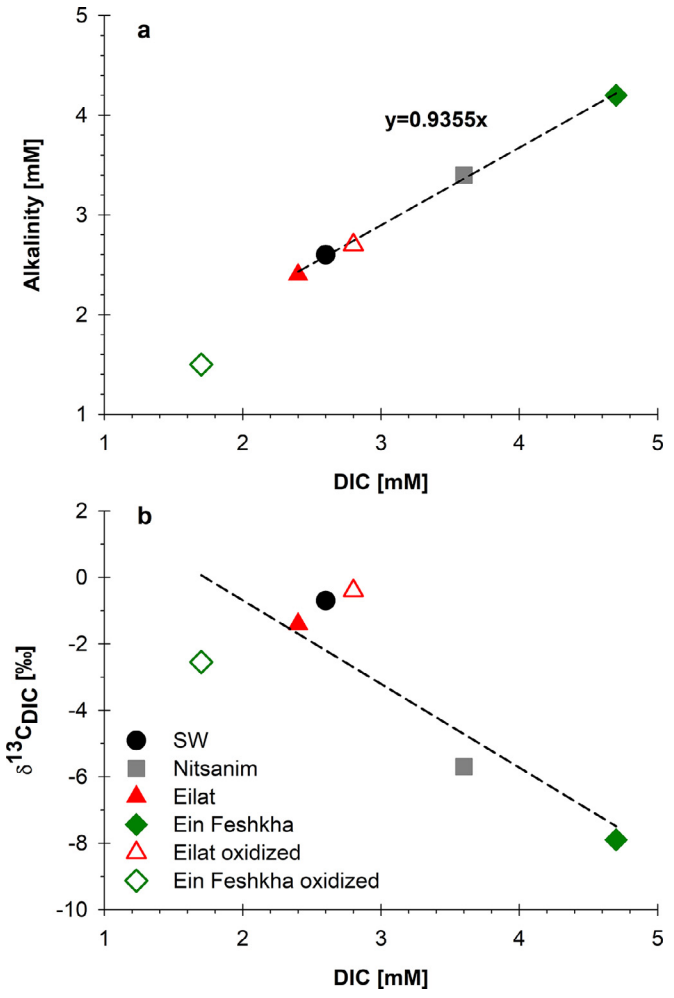

Fig. 3. Alkalinity against DIC (a) and $\delta^{13}C$ against DIC (b) of the three coastal aquifers, the oxidized forms and the Mediterranean seawater of Ashkelon (SW). The trend in (a) represents the natural (reduced) water types excluding the oxidized samples.

Compared with the relative concentrations of Ca^{2+} in the seawater samples, those in the SGWs of Nitsanim and Eilat were enriched, exhibiting increases from 11.45 mM in the Mediterranean Sea to 15.2 mM in Nitsanim and from 12.2 mM in the Gulf of Aqaba (Lazar et al., 2004) to 15.2 mM in Eilat groundwater. Na^{+} showed the opposite trend, and it was depleted in the SGWs of Nitsanim and Eilat (460 mM and 325 mM, respectively) compared with seawater concentrations in the Mediterranean Sea and in the Red Sea (592 mM and 561 Mm, respectively (Al Ouran, 2005)), which were 6% and 10% below conservative mixing. These processes of depletion and enrichment are caused mainly by cation exchange in aquifers due to salinization and freshening events (Russak and Sivan, 2010). Other geochemical processes, such as the dissolution and precipitation of minerals (e.g., $CaCO_3$), which occur during salinization or freshening events, affect also the chemical composition of the water (Andersen et al., 2005; Barker et al., 1998; Magaritz and Luzier, 1985; Price and Herman, 1991; Russak and Sivan, 2010; Wicks et al., 1995; Wicks and Herman, 1996). At Ein Feshkha, the discrepancies between the SGW and seawater concentrations of various ions due to simple mixing in the aquifer may possibly be attributed to the precipitation of different minerals such as gypsum (Kiro et al., 2013), celestine and barite (Kiro et al., 2012) in the FSI zone.

An additional process that has marked effect on the ion compositions of the different groundwater types is biogeochemical-mediated organic matter oxidation. In many SGWs, it has been shown that intensive organic matter oxidation by oxygen leads to its depletion and subsequently suboxic to anoxic conditions. Indeed, the oxygen levels measured in each of our studied aquifers were from 0 to 0.13 mg L^{-1}, and the obtained ORP values were negative (−60 - −230 mV; Table 1). The negative ORP values found in Ein Feshkha were the lowest of the sample sites, followed by Eilat and then Nitsanim, and all of the sites exhibited anaerobic respiration processes. Anaerobic oxidation of organic matter releases HCO_3^-, thus elevating the DIC concentration and alkalinity by the same ratio. Aerobic oxidation of organic matter, in contrast, releases mainly CO_2, but has almost no effect on the alkalinity (Sivan et al., 2005). In all three groundwater systems, organic matter was most likely oxidized anaerobically, which was evidenced by the increase in both alkalinity and DIC by a ratio of ~1 (Fig. 3a, the trend corresponds only to the reduced samples). It can also be seen that the increases in alkalinity and DIC were accompanied by lower $\delta^{13}C_{DIC}$ values (Fig. 3b). This association supports intense microbial oxidation of organic carbon, in which the light carbon isotope is preferable (Appelo and Postma, 2005). This suggests that the Ein Feshkha aquifer has the most intense microbial activity of the examined aquifers and that the Eilat site has the lowest microbial activity. Another explanation for the low $\delta^{13}C_{DIC}$ of Ein Feshkha can be attributed to the relative high dilution of the dead sea water (with value of ~0‰) with fresh groundwater (with low value of −10‰) even though it possesses similar salinities with the other coastal aquifers. The total organic carbon (TOC) found in the aquifers also supports the conclusion of intense microbial activity, as the aquifer in Ein Feshkha possessed the highest TOC concentration (2 ppm) relative to the aquifers in Nitsanim (1.12 ppm) and in Eilat (<0.5 ppm; Table 1). The low bacterial activity of the Red Sea coastal aquifer can be explained by the oligotrophic nature of the Red Sea (Reiss and Hottinger, 2012).

The different extents of organic carbon oxidation that led to varied redox conditions observed in the three aquifers may also lead to the dominance of correspondingly different anaerobic microbial respiration processes in the aquifers (Stumm and Morgan, 2012). Previous studies of the Mediterranean coastal aquifer at Nitsanim found that denitrification was the dominant process for anaerobic bacterial respiration (Russak et al., 2015; Sivan et al., 2005). In the current study the concentrations detected for nitrate (80 μM), nitrite (0.9 μM) and ammonium (2.4 μM) matched the redox condition (denitrification) that was found within the FSI zone (Fig. 4 and Table 1). The concentrations of ammonium and nitrite in the SGW were higher than their concentrations in seawater. This is expected for anaerobic conditions when ammonium is not oxidized and denitrification takes place (nitrite is an intermediate species in this process). Furthermore, ferrous and manganese were not detected in the SGW of Nitsanim, and the sulfate concentration was that expected from simple mixing (dilution) of seawater (Fig. 4a), implying that the redox stage in this aquifer had only reached denitrification and not sulfate reduction.

The aquifer in Eilat showed no depletion in sulfate and no dissolved iron or manganese. Moreover, it contained 50 μM of nitrate, 0.47 μM of nitrite and 0.58 μM of ammonium (Table 1). These findings suggest the presence of mutual microbial nitrification and denitrification processes, but these occur at low rates due to the low organic matter content of the groundwater.

In the Ein Feshkha coastal aquifer, nitrogen compounds comprised a very low concentration of nitrate (0.1 μM), a high concentration of ammonium (4.5 μM) and a relatively high concentration of nitrite (0.6 μM; Table 1, Fig. 4b-d). These findings suggest that the redox conditions enable the occurrence of denitrification. However, dissolved manganese (1.4 μM) and iron (4.3 μM)

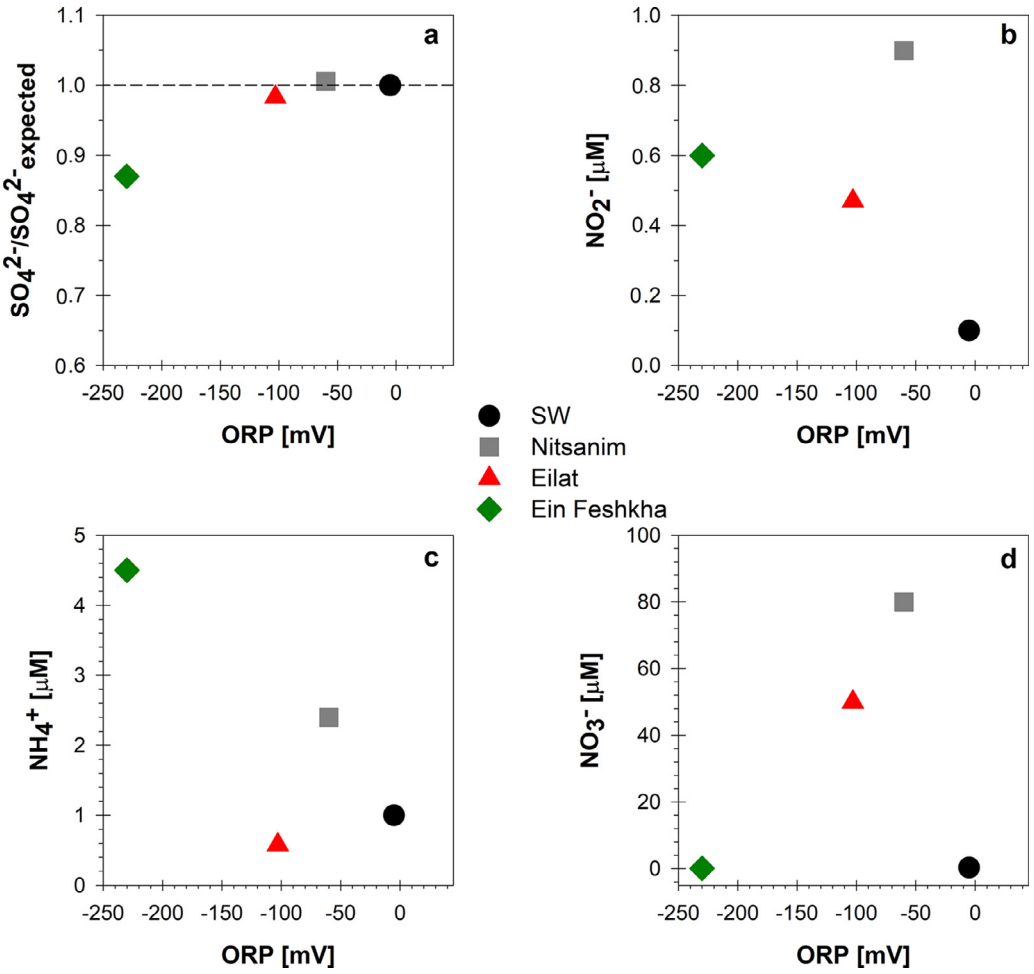

Fig. 4. Sulfate concentration divided by the expected concentration from simple mixing between freshwater and seawater (a), nitrite (b), ammonium (c), and nitrate concentration (d) of the Nitsanim, Eilat and Ein Feshkha coastal aquifers and Mediterranean seawater against oxidation–reduction potential (ORP). The freshwater chemical composition of the Dead Sea coastal aquifer is taken from (Burg et al., 2016) and the saline composition of the Dead Sea is taken from (Reznik et al., 2009). The calculation of the Dead Sea mixing factor was taken from (Avrahamov et al., 2014). The NO_2^- concentration of Mediterranean seawater was taken from (Krom et al., 2005) and the NO_3^- and NH_4^+ concentrations of Mediterranean seawater were taken from (Sivan et al., 2005). Red Sea ion concentrations were taken from (Reznik et al., 2012).

were also found at this site, indicating that the redox stage has reached reduction of manganese and iron oxides. Furthermore, the sulfide concentration of 32.2 μM and a sulfate concentration that was lower than expected from simple mixing of Dead Sea water (Fig. 4a) imply that sulfate reduction is occurring. Although the coexistence of sulfide and Fe^{2+} is uncommon due to their tendency to precipitate as iron monosulfide and pyrite (Canfield, 1989; Kraal et al., 2013), previous studies reported their coexistence in other coastal aquifers (e.g., Georgia, Delaware and South Korea) (Kim et al., 2014; McAllister et al., 2015; Snyder et al., 2004). Yet another study showed, by measuring methane and sulfate concentrations and their isotopes, that sulfate reduction in the Dead Sea coastal aquifer was coupled to the anaerobic oxidation of methane (Avrahamov et al., 2014), which in this aquifer may be produced in deep layers (Avrahamov et al., 2015). It can therefore be concluded that the redox stage of the Ein Feshkha aquifer has favored sulfate reduction.

3.2. RO desalination and fouling experiments with the different water types

Fouling experiments were conducted in the RO cross-flow filtration system (Fig. 2) to evaluate the fouling potential of seawater and of the SGW sampled from the different coastal aquifers. The desalination experiments with the three SGW types were conducted in their natural anaerobic conditions by keeping the water samples under nitrogen atmosphere during the experiment. Furthermore, the oxidized SGW of Ein Feshkha and Eilat were tested as well to determine the potential outcome of oxidation of the feed water prior to the desalination process. Flat-sheet commercial RO membranes (SW30HR membrane) were first compacted with a NaCl solution for 24 h with 50 bars of pressure and initial flux of ~30 L m^{-2} h^{-1}. The filtration experiments of the different water types started with an initial permeate flux (J_0) of 29.8 ± 3.6% L m^{-2} h^{-1} by adjusting the applied pressure due to the difference in water salinities, and the permeate flux over time was recorded at constant pressure. The results from the seawater experiment showed that the permeate flux declined from the initial value to an average of 20.1 L m^{-2} h^{-1} (J/J_0 of 0.75) during 8 h, which represents a 34% reduction (Fig. 5).

The desalination with all the SGW types showed better performance than that with seawater as a result of the lower fouling propensity of the SGW compared to that of the seawater, which resulted in accordingly smaller reductions in flux under SGW desalination. The experiment with the SGW from the Mediterranean coastal aquifer (Nitsanim) showed a permeate flux decline of 10% (Fig. 5). The higher fouling propensity of Mediterranean seawater compared with the low fouling propensity of SGW from the nearby coastal aquifer (Nitsanim) was observed in a previous study

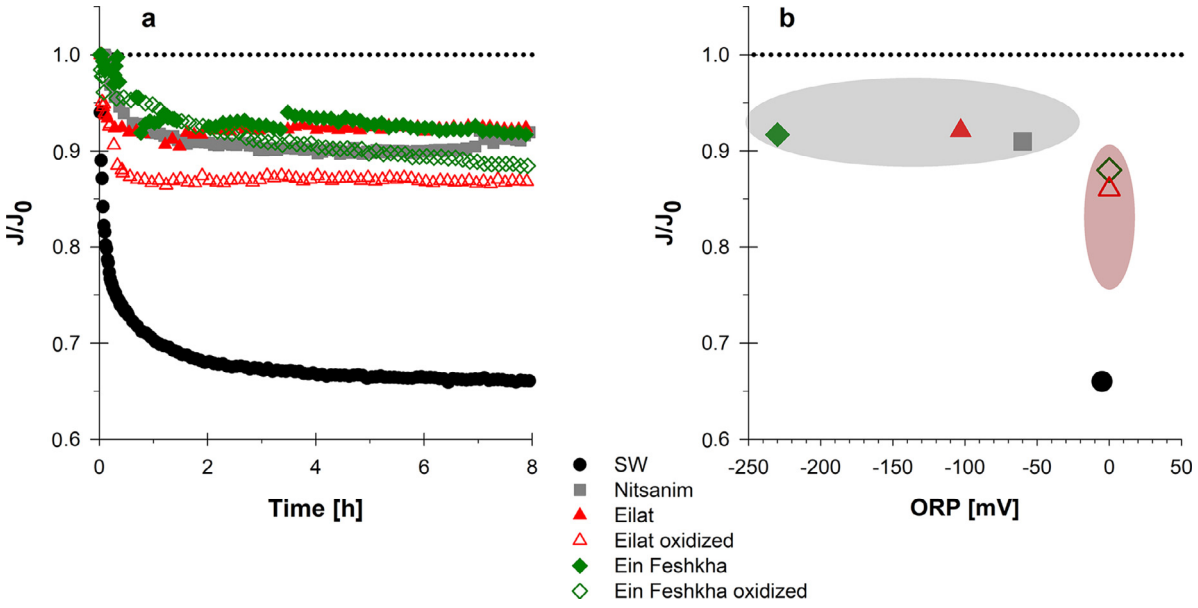

Fig. 5. RO filtration experiments of the different water types. (a) Permeate flux normalized to the initial permeate flux (J/J_0) during 8 h. (b) The normalized permeate flux after 8 h of operation against the oxidation–reduction potential (ORP). The gray ellipse marks the natural groundwater types and the red ellipse marks the oxidized groundwaters. Experiments with natural SGW and experiments after 24 h of SGW oxidation are represented by solid and hollow symbols, respectively.

(Stein et al., 2016) and is in agreement with the flux decline observed in the current study. The experiment with the SGW from the Red Sea coastal aquifer (Eilat) showed a flux reduction of 8% (Fig. 5). The experiment with the SGW from the Dead Sea coastal aquifer (Ein Feshkha) stabilized at an average normalized flux of 0.92, which is an 8% reduction from the initial flux as in the Eilat aquifer. Despite the different redox stages of the Nitsanim and Eilat SGWs compared to that of the Ein Feshkha SGW, all three aquifers showed generally the same reduction in flux. The lower fouling propensity of SGW is a major benefit of using it rather than seawater as the feed for desalination: the lower applied pressure required in SGW desalination translates into reduced energy demand, less membrane cleaning and lower operational costs.

Evaluation of the SDI values for the SGW of Nitsanim, Eilat and Ein Feshkha showed 4.6, 5.44 and 0.91% min^{-1}, respectively, which are lower than the SDI of seawater (6.35% min^{-1}; Table 1). A sensitive parameter, SDI can be used to predict fouling potential (Mosset et al., 2008), and indeed, in this study the seawater had a higher SDI and showed a higher fouling propensity than the SGW samples. In some cases, such as in Almeria and Saudi Arabia, the natural filtration of the aquifer reduces the SDI values by more than 90% (Rachman et al., 2014; Sola et al., 2013). Other possible causes for the higher fouling of seawater compared with that of SGW are the oxygen levels and the presence of transparent exopolymer particles that are secreted by marine microorganisms in seawater (Bar-Zeev et al., 2009). The lower oxygen levels in SGW than in seawater (Table 1) is beneficial, as it inhibits biofilm production on the membrane and was shown to prolong membrane life span (Beyer et al., 2014). In our experiment, although significant biofouling is not expected during the operation of the RO experiments, the potentially reduced biofouling propensity of SGW may be an additional important advantage for continuous RO desalination practices.

The SGWs of Eilat and Ein Feshkha were oxidized by opening the tank and stirring for 24 h, after which the DO of the water was at saturation. RO filtration experiments were then conducted with the oxidized waters. The experiment with the oxidized water of Eilat showed a permeate flux decline that reached an average flux of 27.1 L m^{-2} h^{-1}, which is a 13% reduction from the initial flux (J/J_0 of 0.87; Fig. 5). The flux decline of the oxidized SGW of Eilat was larger than the flux decline found for the natural (reduced) water of Eilat. Permeate flux during the RO filtration of the Ein Feshkha oxidized water was reduced to 26.6 L m^{-2} h^{-1} (J/J_0 of 0.88), which is a 12% reduction in flux (Fig. 5). Similar to our findings for the oxidized Eilat water, in tests of the Ein Feshkha water a greater reduction in flux was obtained with the oxidized compared with the natural (reduced state) water. The higher fouling levels observed for the oxidized compared with the natural (reduced) waters of both Eilat and Ein Feshkha imply that the redox stages of the waters may influence their fouling propensities in the RO desalination process.

The oxidation of naturally reduced water can cause precipitation due to changes in the solution chemistry where reduced species that are naturally dissolved may precipitate due to the change of their oxidation state. Also, the enhanced fouling and scaling of the oxidized waters can be attributed to the increased pH values of the two aquifer waters. The natural pH values of Eilat and Ein Feshkha are 7.06 and 6.75, respectively, while after the oxidation process, those values were elevated to 7.5 and 7.7, respectively. These observed increases in pH, which are attributed to CO_2 release to the atmosphere during the oxidation stage, may cause mineral precipitation especially of carbonates, whose solubility decreases at high pH values. Indeed, $CaCO_3$ precipitation was observed in the water tank (confirmed by X-ray diffraction (XRD) analysis; Fig. S1) during the 24 h oxidation of the Ein Feshkha water, which exhibited the largest change in pH. The Ca^{2+} and the DIC concentrations of the oxidized Ein Feshkha water were lower than in the natural (reduced) form (Table 1), findings that are in agreement with the $CaCO_3$ precipitation. Hence, both the change in the redox stage and with the increase in pH upon oxidation contributed to the increased fouling propensity of the oxidized water.

3.3. Characteristics of the fouling layer on the RO membranes

To study the fouling properties of each water type, the fouled membranes from each experiment were examined. The ionic compositions of the foulants were determined by dissolving the precipitates in a fixed volume of nitric acid followed by ICP measurement. The membrane of the seawater desalination experiment

Table 2
ICP analysis of the precipitates on the fouled membranes after precipitate dissolution in 1 M nitric acid. Data are presented in μg cm^{-2} of the membrane.

Element	SW	Nitsanim	Eilat	Eilat oxidized	Ein Feshkha	Ein Feshkha oxidized
Ca^{2+}	3.8	6.5	5.1	1.7	16.1	26.0
Fe	2.0	0.5	0.9	1.6	1.1	0.9
K^{+}	3.9	2.9	1.4	0.1	4.1	6.4
Mg^{2+}	9.6	6.4	2.9	1.9	16.5	25.8
S	5.5	3.7	2.9	1.4	0.4	0.7
Si	26.1	12.0	2.8	1.0	6.5	6.6

Table 3
Saturation index calculated by PHREEQC software for various minerals in the different water types and the concentration polarization evaluations for the RO filtration system when using each water type to predict the possible mineral precipitates during RO desalination.

Mineral	Chemical composition	SW	Nitsanim	Eilat	Eilat oxidized	Ein Feshkha	Ein Feshkha oxidized
Concentration polarization [a]		2.2	1.9	2.6	2.3	3.5	2.9
Ca minerals							
Aragonite	$CaCO_3$	1.18	0.72	0.61	0.96	0.96	1.22
Calcite	$CaCO_3$	1.46	1	0.89	1.24	1.24	1.5
Gypsum	$CaSO_4{\cdot}2H_2O$	−0.66	−0.67	−0.36	−0.43	−0.95	−1.09
Huntite	$CaMg_3(CO_3)_4$	5.38	2.59	1.69	3.11	3.7	4.83
Si minerals							
Talc	$Mg_3Si_4O_{10}(OH)_2$		3.12	2.44	4.78	3.08	8
Antigorite	$Mg_{48}Si_8O_{22}(OH)_2$		27.42	6.81	45.44	6.86	89.03
Anthophyllite	$Mg_7Si_{34}O_{85}(OH)_{62}$		−4.57	−6.59	−1.09	−5.52	6.09
Sepiolite	$Mg_4Si_6O_{15}(OH)_5{\cdot}6H_2O$		−0.71	−1.04	0.51	−0.53	2.72
Quartz	SiO_2		0.23	0.56	0.51	0.89	0.77
Fe minerals							
Goethite	FeO(OH)					7.87	
Mackinawite	Fes					0.23	
Pyrite	FeS_2					23.84	
Magnesite	$MgCO_3$	1.6	0.83	0.56	0.92	1.11	1.4
Sulfur	S	−56	−50.5	−47.66	−51.2	11.84	10.57

[a] Calculation of concentration polarization is presented in the supporting information.

showed a high silicon content and relatively high levels of sulfur, iron and magnesium (Table 2). Silicon and iron were also observed by surface elemental analysis (by XPS) of the seawater membrane (Table S1). The observation that silicon and iron were observed in high concentrations on the fouled membrane, but were below the detection limit in the feed seawater indicates their being aggregated and concentrated on the membrane during the RO filtration process. Other studies detected silicate and iron fouling during seawater desalination (Aubry et al., 2014; Li et al., 2012), and in some cases, the fouling resulted from the dissolved ionic forms of silicates and iron (Li et al., 2012) when these were present. Recent review articles indicated that the most common foulant types of seawater RO desalination are colloidal iron and silica (Badruzzaman et al., 2019; Jiang et al., 2017). Generally, iron fouling on RO membranes is mostly colloidal, usually as silicates (Ning, 2009).

The foulant composition of the membrane used in the Nitsanim natural (reduced) SGW experiment showed high contents of silicon, calcium and magnesium (Table 2). In this case, it is plausible that colloidal magnesium silicates were the dominant foulants due to the sand-stone dominance in this aquifer.

The fouling layer of the Eilat (reduced) SGW RO experiment was dominated by calcium, and it had relatively equal depositions of magnesium, sulfur and silicon. Calcium, sulfur and silicon were also detected by the XPS surface analysis (Table S1). These elements probably originated from the magmatic and metamorphic crystalline host rocks of the alluvial aquifer in Eilat. SEM analysis shows depositions of aluminosilicates with high iron content, including iron particles in the μm size range (Fig. S2). The ionic profiles of the membrane depositions from the RO experiment with the oxidized Eilat water were similar to those of its natural (reduced) form (Table 2), and SEM analysis detected particle deposition with the above elements (Fig. S3). The oxidation of the Eilat water did not substantially change the chemical composition of the feed water (Table 1), which is in agreement with similar fouling properties of Eilat natural and oxidized waters.

The membrane from the RO experiment with the Ein Feshkha natural water was fouled mainly with calcium and magnesium with silicon deposits (Table 2). XPS surface analysis shows a similar trend of finding calcium, magnesium and silicon on the membrane (Table S1). The fouled membrane from the experiment of oxidized Ein Feshkha water shows a similar deposition pattern, namely, mostly calcium and magnesium with additional silicon, but in this case, the calcium and magnesium were present in much higher concentrations (Table 2). This finding is probably due to the formation of calcium and magnesium precipitates in the oxidized groundwater, as discussed above for $CaCO_3$, and it agrees with the more intense fouling observed for the oxidized water (Fig. 5). Ferrous iron is often observed in anoxic groundwaters, but when these are exposed to the partial pressure of oxygen in the atmosphere, it is oxidized and precipitates as ferric hydroxide within minutes to hours (Sung and Forbes, 1984). In the natural (reduced) Ein Feshkha water, iron was in its dissolved-reduced form; however, oxidation of the water did not significantly increase the level of iron deposition on the membrane, probably due to its low concentration in the bulk Ein Feshkha water (~4 μM; Table 1). Sulfur was detected in higher concentrations on the membrane of the oxidized experiment compared with the natural (reduced) form of the Ein Feshkha water. This may be due to the behavior of dissolved reduced sulfur (sulfide, as HS^{-}, 32.2 μM in Ein Feshkha SGW; Table 1) and the deposition of elemental sulfur when oxidized. A coastal aquifer in Delaware Bay was found to have dissolved ferrous iron concentrations of ~1000 μM and sulfide concentrations of up to 466 μM (McAllister et al., 2015) that, upon ox-

idation, may strongly precipitate. These findings indicate that the redox stage of coastal aquifers may have a marked impact on RO processes. Therefore, to predict the potential fouling and associated challenges of applying the RO system in the treatment of saline groundwaters, it is essential that the concentrations of the redox species present in the water, and their dynamics, be accurately measured and fully understood. Ning et al. showed that running an RO desalination plant with feed water from an aquifer in Bahrein that contained 90 µM of sulfide resulted in severe elemental sulfur fouling within two days of starting operation (Ning et al., 2005).

Saturation index calculations for different minerals in the studied water types were performed by PHREEQC software (Parkhurst and Appelo, 1999) taking into account the concentration polarization in the RO system used for the filtration experiments (Table 3). In addition, the SI includes further explanation about the calculations for concentration polarization and salt rejection (Fig. S2). In general, almost all of the minerals presented in Table 3 had higher saturation index values for the oxidized SGW than for the natural (reduced) form. All water types exhibited a tendency for the precipitation of $CaCO_3$ (aragonite and calcite) and calcium magnesium carbonate (huntite - $CaMg_3(CO_3)_4$). Thus, scaling by these minerals can explain the calcium and magnesium deposits that were found on all membranes. Silicate minerals such as talc, antigorite and quartz were each found to have a positive saturation index in all experiments besides those with seawater, because silicon was not detected in the seawater. Thus, silicates are a potential scaling factor in the SGW desalination process. In the oxidized Ein Feshkha water, the silicate mineral anthophyllite was found to have a positive saturation index. Interestingly, iron minerals such as goethite and pyrite had high positive saturation index values in the natural (reduced) Ein Feshkha water. Elemental sulfur deposition is likely to occur both in Ein Feshkha natural water and in its oxidized form, which had sulfide concentrations of 32.2 and 1.53 µM, respectively. SEM analyses indicated the presence of sulfur dominated spots on the membranes used for the natural and oxidized Ein Feshkha water filtrations (Figures S4 and S5).

4. Conclusions

The findings of this work show how the natural redox stage of SGWs from coastal aquifers affects the performance of RO desalination. In addition, this study demonstrates the benefits of SGW desalination over seawater desalination. The natural reducing conditions of the SGW have major implications for the RO process as it results in a lower fouling propensity compared with the oxidized form of the water and the seawater. Maintenance of the natural reducing stage of the water may prevent precipitation by keeping the iron and sulfur species in their reduced, dissolved forms and by reducing the saturation index of relevant minerals, thereby reducing the membrane scaling phenomenon. One of the principal conclusions from this study, therefore, is the importance of preventing the feed water from being exposed to atmospheric conditions due to their potential oxidation, and to CO_2 release and a subsequent rise in pH that was shown to enhance mineral precipitation. Keeping the groundwater in its natural state will reduce the total cost of the RO process as the need for feed stream pretreatments is reduced significantly.

This work shows that low redox stage of the feed water improves desalination performance. Reduced conditions cause less fouling, where different redox levels of anaerobic natural waters have comparable RO system performance. The SGWs from Nitsanim and Eilat were found to be in a denitrification stage, while Ein Feshkha was in a sulfate reduction stage, but all three water types showed comparable fouling propensities (Fig. 5b). Using naturally reduced SGWs from coastal aquifers as the feed water for RO desalination may result in reduced membrane fouling, thus ameliorating the associated problems and costs typically encountered during RO process operation. These findings, together with the lower salinity of the SGW relative to seawater, indicate that the use of SGW in RO desalination systems may reduce the energy demand and overall operational costs of the RO process.

Declaration of Competing Interest

The authors declare that they have no known competing financial interests or personal relationships that could have appeared to influence the work reported in this paper.

Acknowledgments

We are grateful to Nathalia Frumin and Ana Millionshchick from the Ilse Katz Institute for Nanoscale Science and Technology, Ben-Gurion University of the Negev for the XRD, XPS and SEM analyses. We thank Alon Moshe, Iyad Swaed and Uria Va'anunu from the Geological Survey of Israel for their help in the field. We would like to thank also the reviewers and the editor for their constructive remarks. S. S. was a recipient of the Negev Fellowship from the Kreitmann School at Ben-Gurion University of the Negev. We thank also the Rieger foundation – JNF for their generous support to S.S.

Supplementary materials

Supplementary material associated with this article can be found, in the online version, at doi:10.1016/j.watres.2020.116508.

References

Al Ouran,, N., 2005. Environmental Assessment, Documentation and Spatial Modeling of Heavy Metal Pollution along the Jordan Gulf of Aqaba Using Coral Reefs As Environmental Indicator Umweltbewertung. Dokumentation und räumliche Modellierung der Schwermetallverschmutzung ent. Dep. Hydrogeol. Environ. Julius-Maximilians-University Würzbg.

Amy, G., Ghaffour, N., Li, Z., Francis, L., Linares, R.V., Missimer, T., Lattemann, S., 2017. Membrane-based seawater desalination: present and future prospects. Desalination 401, 16–21. https://doi.org/10.1016/j.desal.2016.10.002.

Andersen, M.S., Nyvang, V., Jakobsen, R., Postma, D., 2005. Geochemical processes and solute transport at the seawater/freshwater interface of a sandy aquifer. Geochim. Cosmochim. Acta 69, 3979–3994. https://doi.org/10.1016/j.gca.2005.03.017.

Appelo, C.A.J., Postma, D., 2005. Geochemistry, Groundwater and Pollution, 2nd edition.

Aubry, C., Khan, M.T., Behzad, A.R., Anjum, D.H., Gutierrez, L., Croue, J.P., 2014. In: Cross-sectional Analysis of Fouled SWRO Membranes By STEM-EDS. Desalination, 333, pp. 118–125.

Avrahamov, N., Antler, G., Yechieli, Y., Gavrieli, I., Joye, S.B., Saxton, M., Turchyn, A.V., Sivan, O., 2014. Anaerobic oxidation of methane by sulfate in hypersaline groundwater of the Dead Sea aquifer. Geobiology 12, 511–528. https://doi.org/10.1111/gbi.12095.

Avrahamov, N., Gelman, F., Yechieli, Y., Aizenshtat, Z., Nissenbaum, A., Sivan, O., 2015. Proposed sources of methane along the dead sea transform. Chem. Geol. 395, 165–175. https://doi.org/10.1016/j.chemgeo.2014.11.026.

Avrahamov, N., Yechieli, Y., Lazar, B., Lewenberg, O., Boaretto, E., Sivan, O., 2010. Characterization and dating of saline groundwater in the dead sea area. Radiocarbon 52, 1123–1140. https://doi.org/10.1017/S0033822200046208.

Badruzzaman, M., Voutchkov, N., Weinrich, L., Jacangelo, J.G., 2019. Selection of pretreatment technologies for seawater reverse osmosis plants: a review. Desalination 449, 78–91. https://doi.org/10.1016/j.desal.2018.10.006.

Bar-Zeev, E., Berman-Frank, I., Liberman, B., Rahav, E., Passow, U., Berman, T., 2009. Transparent exopolymer particles: potential agents for organic fouling and biofilm formation in desalination and water treatment plants. Desalin. Water Treat. 3, 136–142. https://doi.org/10.5004/dwt.2009.444.

Barker, A.P., Newton, R.J., Bottrell, S.H., Tellam, J.H., 1998. Processes affecting groundwater chemistry in a zone of saline intrusion into an urban sandstone aquifer. Appl. Geochem. 13, 735–749. https://doi.org/10.1016/S0883-2927(98)00006-7.

Beyer, F., Rietman, B.M., Zwijnenburg, A., Brink, P., Van Den, Vrouwenvelder, S., Jarzembowska, M., Laurinonyte, J., Stams, A.J.M., Plugge, C.M., 2014. Long-term performance and fouling analysis of full-scale direct nano filtration (NF) installations treating anoxic groundwater. J. Memb. Sci. 468, 339–348. https://doi.org/10.1016/j.memsci.2014.06.004.

Burg, A., Yechieli, Y., Galili, U., 2016. Response of a coastal hydrogeological system to a rapid decline in sea level; the case of Zuqim springs - The largest discharge area along the Dead Sea coast. J. Hydrol. 536, 222–235. https://doi.org/10.1016/j.jhydrol.2016.02.039.

Canfield, D.E., 1989. Reactive iron in marine sediments. Geochim. Cosmochim. Acta 53, 619–632. https://doi.org/10.1016/0016-7037(89)90005-7.
Charette, M.A., Sholkovitz, E.R., Hansel, C.M., 2005. Trace element cycling in a subterranean estuary: part 1. Geochemistry of the permeable sediments. Geochim. Cosmochim. Acta 69, 2095–2109. https://doi.org/10.1016/j.gca.2004.10.024.
Chen, J., Gu, B., Royer, R.A., Burgos, W.D., 2003. The roles of natural organic matter in chemical and microbial reduction of ferric iron. Sci. Total Environ. 307, 167–178. https://doi.org/10.1016/S0048-9697(02)00538-7.
Cline, J.D., 1969. Spectrophotometric determination of hydrogen sulfide in natural waters. Limnol. Oceanogr. 14, 454–458. https://doi.org/10.4319/lo.1969.14.3.0454.
Connor, A.E.O., Luek, J.L., Mcintosh, H., Beck, A.J., 2015. Geochemistry of redox-sensitive trace elements in a shallow subterranean estuary. Mar. Chem. 172, 70–81. https://doi.org/10.1016/j.marchem.2015.03.001.
Dehwah, A.H.A., Missimer, T.M., 2016. Subsurface intake systems: green choice for improving feed water quality at SWRO desalination plants. Jeddah, Saudi Arabia. Water Res. 88, 216–224. https://doi.org/10.1016/j.watres.2015.10.011.
Duncan, T., Shaw, T.J., 2003. The mobility of Rare Earth Elements and Redox Sensitive Elements in the groundwater/seawater mixing zone of a shallow coastal aquifer. Aquat. Geochem. 9, 233–255. https://doi.org/10.1023/B:AQUA.0000022956.20338.26.
Greve, P., Kahil, T., Mochizuki, J., Schinko, T., Satoh, Y., Burek, P., Fischer, G., Tramberend, S., Burtscher, R., Langan, S., Wada, Y., 2018. Global assessment of water challenges under uncertainty in water scarcity projections. Nat. Sustain. 1, 486–494. https://doi.org/10.1038/s41893-018-0134-9.
Hoekstra, A.Y., Mekonnen, M.M., 2012. The water footprint of humanity. Proc. Natl. Acad. Sci. 109, 3232–3237. https://doi.org/10.1073/pnas.1109936109.
Houben, G., Post, V.E.A., 2017. The first field-based descriptions of pumping-induced saltwater intrusion and upconing. Hydrogeol. J. 25, 243–247. https://doi.org/10.1007/s10040-016-1476-x.
Jiang, S., Li, Y., Ladewig, B.P., 2017. A review of reverse osmosis membrane fouling and control strategies. Sci. Total Environ. 595, 567–583. https://doi.org/10.1016/j.scitotenv.2017.03.235.
Kim, D., Yun, S., Jae, M., Mayer, B., Kim, K., 2014. Assessing redox zones and seawater intrusion in a coastal aquifer in South Korea using hydrogeological, chemical and isotopic approaches. Chem. Geol. 390, 119–134. https://doi.org/10.1016/j.chemgeo.2014.10.024.
Kiro, Y., Weinstein, Y., Starinsky, A., Yechieli, Y., 2013. Groundwater ages and reaction rates during seawater circulation in the Dead Sea aquifer. Geochim. Cosmochim. Acta 122, 17–35. https://doi.org/10.1016/j.gca.2013.08.005.
Kiro, Y., Yechieli, Y., Voss, C.I., Starinsky, A., Weinstein, Y., 2012. Modeling radium distribution in coastal aquifers during sea level changes: the Dead Sea case. Geochim. Cosmochim. Acta 88, 237–254. https://doi.org/10.1016/j.gca.2012.03.022.
Kraal, P., Burton, E.D., Bush, R.T., 2013. Iron monosulfide accumulation and pyrite formation in eutrophic estuarine sediments. Geochim. Cosmochim. Acta 122, 75–88. https://doi.org/10.1016/j.gca.2013.08.013.
Krom, M.D., Woodward, E.M.S., Herut, B., Kress, N., Carbo, P., Mantoura, R.F.C., Spyres, G., Thingsted, T.F., Wassmann, P., Wexels-Riser, C., Kitidis, V., Law, C., Zodiatis, G., 2005. Nutrient cycling in the south east Levantine basin of the eastern Mediterranean: results from a phosphorus starved system. Deep. Res. Part II Top. Stud. Oceanogr. 52, 2879–2896. https://doi.org/10.1016/j.dsr2.2005.08.009.
Lazar, B., Enmar, R., Schossberger, M., Bar-Matthews, M., Halicz, L., Stein, M., 2004. Diagenetic effects on the distribution of uranium in live and Holocene corals from the Gulf of Aqaba. Geochim. Cosmochim. Acta 68, 4583–4593. https://doi.org/10.1016/j.gca.2004.03.029.
Li, Z.Y., Yangali-Quintanilla, V., Valladares-Linares, R., Li, Q., Zhan, T., Amy, G., 2012. Flux patterns and membrane fouling propensity during desalination of seawater by forward osmosis. Water Res 46, 195–204. https://doi.org/10.1016/j.watres.2011.10.051.
Magaritz, M., Luzier, J.E., 1985. Water-rock interactions and seawater-freshwater mixing effects in the coastal dunes aquifer, Coos Bay, Oregon. Geochim. Cosmochim. Acta 49, 2515–2525. https://doi.org/10.1016/0016-7037(85)90119-X.
McAllister, S.M., Barnett, J.M., Heiss, J.W., Findlay, A.J., MacDonald, D.J., Dow, C.L., Luther, G.W., Michael, H.A., Chan, C.S., 2015. Dynamic hydrologic and biogeochemical processes drive microbially enhanced iron and sulfur cycling within the intertidal mixing zone of a beach aquifer. Limnol. Oceanogr. 60, 329–345. https://doi.org/10.1111/lno.10029.
Michael, H.A., Mulligan, A.E., Harvey, C.F., 2005. Seasonal oscillations in water exchange between aquifers and the coastal ocean. Nature 436, 1145–1148. https://doi.org/10.1038/nature03935.
Mosset, A., Bonnelye, V., Petry, M., Sanz, M.A., 2008. The sensitivity of SDI analysis: from RO feed water to raw water. Desalination 222, 17–23. https://doi.org/10.1016/j.desal.2007.01.125.
Nederlof, M.M., Kruithof, J.C., Taylor, J.S., Van Der Kooij, D., Schippers, J.C., 2000. Comparison of NF/RO membrane performance in integrated membrane systems. Desalination 131, 257–269. https://doi.org/10.1016/S0011-9164(00)90024-9.
Ning, R.Y., 2009. Colloidal iron and manganese in water affecting RO operation. Desalin. Water Treat. 12, 162–168. https://doi.org/10.5004/dwt.2009.918.
Ning, R.Y., Troyer, T.L., Tominello, R.S., 2005. Chemical control of colloidal fouling of reverse osmosis systems. Desalination 172, 1–6. https://doi.org/10.1016/j.desal.2004.06.192.
Parkhurst, D.L., Appelo, C.A.J., 1999. User's Guide To PHREEQC (Version 2)- A Computer Program For Speciation, Batch-Reaction, One-Dimensional Transport, And Inverse Geochemical Calculations. U.S. Geological Survey. U.S. Department Of The Interior, Denver, Colorado https://doi.org/10.2307/3459821.
Porubsky, W.P., Weston, N.B., Moore, W.S., Ruppel, C., Joye, S.B., 2014. Dynamics of submarine groundwater discharge and associated fluxes of dissolved nutrients, carbon, and trace gases to the coastal zone (Okatee River estuary, South Carolina). Geochim. Cosmochim. Acta 131, 81–97. https://doi.org/10.1016/j.gca.2013.12.030.
Price, R.M., Herman, J.S., 1991. Geochemical investigations of saltwater intrusion into the coastal carbonate aquifer of Mallorca. Spain. Appl. Geochemistry 103, 1270–1279. https://doi.org/10.1016/j.apgeochem.2013.09.011.
Rachman, R.M., Li, S., Missimer, T.M., 2014. SWRO feed water quality improvement using subsurface intakes in Oman, Spain, Turks and Caicos Islands, and Saudi Arabia. Desalination 351, 88–100. https://doi.org/10.1016/j.desal.2014.07.032.
Reiss, Z., Hottinger, L., 2012. The Gulf of Aqaba: Ecological Micropaleontology, 50. Springer science & Business media.
Reznik, I.J., Ganor, J., Gruber, C., Gavrieli, I., 2012. Towards the establishment of a general rate law for gypsum nucleation. Geochim. Cosmochim. Acta 85, 75–87. https://doi.org/10.1016/j.gca.2012.02.002.
Reznik, I.J., Gavrieli, I., Ganor, J., 2009. Kinetics of gypsum nucleation and crystal growth from Dead Sea brine. Geochim. Cosmochim. Acta 73, 6218–6230. https://doi.org/10.1016/j.gca.2009.07.018.
Roy, M., Martin, J.B., Cherrier, J., Cable, J.E., Smith, C.G., 2010. Influence of sea level rise on iron diagenesis in an east Florida subterranean estuary. Geochim. Cosmochim. Acta 74, 5560–5573. https://doi.org/10.1016/j.gca.2010.07.007.
Russak, A., Sivan, O., 2010. Hydrogeochemical tool to identify salinization or freshening of coastal aquifers determined from combined field work, experiments, and modeling. Environ. Sci. Technol. 44, 4096–4102. https://doi.org/10.1021/es1003439.
Russak, A., Yechieli, Y., Herut, B., Lazar, B., Sivan, O., 2015. The effect of salinization and freshening events in coastal aquifers on nutrient characteristics as deduced from field data. J. Hydrol. 529, 1293–1301. https://doi.org/10.1016/j.jhydrol.2015.07.034.
Santos, I.R., Burnett, W.C., Misra, S., Suryaputra, I.G.N.A., Chanton, J.P., Dittmar, T., Peterson, R.N., Swarzenski, P.W., 2011. Uranium and barium cycling in a salt wedge subterranean estuary : the in fl uence of tidal pumping. Chem. Geol. 287, 114–123. https://doi.org/10.1016/j.chemgeo.2011.06.005.
Shahzad, M.W., Burhan, M., Ang, L., Ng, K.C., 2017. Energy-water-environment nexus underpinning future desalination sustainability. Desalination 413, 52–64. https://doi.org/10.1016/j.desal.2017.03.009.
Sim, L.N., Chong, T.H., Taheri, A.H., Sim, S.T.V., Lai, L., Krantz, W.B., Fane, A.G., 2018. A review of fouling indices and monitoring techniques for reverse osmosis. Desalination 434, 169–188. https://doi.org/10.1016/j.desal.2017.12.009.
Sirois, M., Couturier, M., Barber, A., Gélinas, Y., Chaillou, G., 2018. Interactions between iron and organic carbon in a sandy beach subterranean estuary. Mar. Chem. 202, 86–96. https://doi.org/10.1016/j.marchem.2018.02.004.
Sivan, O., Yechieli, Y., Herut, B., Lazar, B., 2005. Geochemical evolution and timescale of seawater intrusion into the coastal aquifer of Israel. Geochim. Cosmochim. Acta 69, 579–592. https://doi.org/10.1016/j.gca.2004.07.023.
Snyder, M., Taillefert, M., Ruppel, C., 2004. Redox zonation at the saline-influenced boundaries of a permeable surficial aquifer: effects of physical forcing on the biogeochemical cycling of iron and manganese. J. Hydrol. 296, 164–178. https://doi.org/10.1016/j.jhydrol.2004.03.019.
Sola, F., Vallejos, A., López-Geta, J.A., Pulido-Bosch, A., 2013. The role of aquifer media in improving the quality of seawater feed to desalination plants. Water Resour. Manag. 27, 1377–1392. https://doi.org/10.1007/s11269-012-0243-6.
Stein, S., Russak, A., Sivan, O., Yechieli, Y., Rahav, E., Oren, Y., Kasher, R., 2016. Saline groundwater from coastal aquifers as a source for desalination. Environ. Sci. Technol. 50. https://doi.org/10.1021/acs.est.5b03634.
Stein, S., Sola, F., Yechieli, Y., Shalev, E., Sivan, O., Kasher, R., Vallejos, A., 2020. The effects of long-term saline groundwater pumping for desalination on the fresh – saline water interface : field observations and numerical modeling. Sci. Total Environ. 732, 139249. https://doi.org/10.1016/j.scitotenv.2020.139249.
Stein, S., Yechieli, Y., Shalev, E., Kasher, R., Sivan, O., 2019. The effect of pumping saline groundwater for desalination on the fresh–saline water interface dynamics. Water Res 46–57. https://doi.org/10.1016/j.watres.2019.03.003.
Stookey, L.L., 1970. Ferrozine-a new spectrophotometric reagent for iron. Anal. Chem. 42, 779–781.
Stumm, W., Morgan, J.J., 2012. Aquatic chemistry: Chemical Equilibria and Rates in Natural waters, Third edit. John Wiley &Sons.
Sung, W., Forbes, E.J., 1984. Some consideration on iron removal. J. Environ. Eng. 110, 1048–1061.
Wicks, C.M., Herman, J.S., Randazzo, A.F., Jee, J.L., 1995. Water-rock interactions in a modern coastal mixing zone. Geol. Soc. Am. Bull. 107, 1023–1032 10.1130/0016-7606(1995)107<1023:WRIIAM>2.3.CO;2.
Wicks, M., Herman, J.S., 1996. Regional hydrogeochemistry of a modern coastal mixing zone. Water Resour. Res. 32, 401–407.
Yechieli, Y., Kafri, U., Sivan, O., 2009. The inter-relationship between coastal subaquifers and the Mediterranean Sea, deduced from radioactive isotopes analysis. Hydrogeol. J. 17, 265–274. https://doi.org/10.1007/s10040-008-0329-7.
Yechieli, Y., Shalev, E., Wollman, S., Kiro, Y., Kafri, U., 2010. Response of the Mediterranean and Dead Sea coastal aquifers to sea level variations. Water Resour. Res. 46, 1–11. https://doi.org/10.1029/2009WR008708.
Yiantsios, S.G., Karabelas, A.J., 2003. An assessment of the Silt Density Index based on RO membrane colloidal fouling experiments with iron oxide particles. Desalination 151, 229–238. https://doi.org/10.1016/S0011-9164(02)01015-9.
Zhou, Q., Bear, J., Bensabat, J., 2005. Saltwater upconing and decay beneath a well pumping above an interface zone. Transp. Porous Media 61, 337–363. https://doi.org/10.1007/s11242-005-0261-4.